Imaging Features of COVID-19-Associated Acute Invasive Fungal Rhinosinusitis

Nishtha Yadav[1] Ambuj Kumar[2] Kavita Sachdeva[3] Shruti Asati[4]

[1] Department of Neuroradiology, Super Speciality Hospital, Netaji Subhash Chandra Bose Medical College Jabalpur, Jabalpur, Madhya Pradesh, India
[2] Department of Neurosurgery, Super Speciality Hospital, Netaji Subhash Chandra Bose Medical College Jabalpur, Jabalpur, Madhya Pradesh, India
[3] Department of ENT, Netaji Subhash Chandra Bose Medical College Jabalpur, Jabalpur, Madhya Pradesh, India
[4] Department of Microbiology, Netaji Subhash Chandra Bose Medical College Jabalpur, Jabalpur, Madhya Pradesh, India

Address for correspondence Nishtha Yadav, MBBS, MD (Radiology), DM (Neuroimaging and Interventional Radiology), Department of Neuroradiology, School of Excellence in Neurosurgery, Super Speciality Hospital, Netaji Subhash Chandra Bose Medical College Jabalpur, Jabalpur, Madhya Pradesh, 482003, India (e-mail: nishthayadavthesis@gmail.com).

Indian J Neurosurg 2023;12:229–239.

Abstract

Background Acute invasive fungal rhinosinusitis (AIFR) is a rare, rapidly progressive, and life-threatening infection involving the nasal cavity and paranasal sinuses. Purpose of this study is to describe imaging features of coronavirus disease-2019 (COVID-19)-associated AIFR.

Methods This was a retrospective observational study. Inclusion criteria: (1) post-COVID-19 patients with fungal rhinosinusitis detected on potassium hydroxide smear or histopathology; (2) onset of symptoms (facial pain, dental pain, facial swelling or discoloration, nasal bleed, periorbital swelling, ptosis, redness of eyes, vision loss) less than 4 weeks; and (3) magnetic resonance imaging/computed tomography (MRI/CT) done within 5 days before surgery. Exclusion criteria: (1) cases of sinusitis without a history of previous COVID-19 infection; and (2) cases in whom fungal hyphae were not demonstrated on pathological examination. Noncontrast CT and dedicated MRI sequences were done initially. Site of involvement, unilateral/bilateral involvement, pattern of mucosal thickening, enhancement pattern, periantral invasion, orbital invasion, intracranial involvement, perineural spread, vascular involvement, and bony involvement were recorded. CT and MRI imaging features were compared.

Results Analysis of 90 studies (CT and MRI) in 60 patients was done. Most common site of involvement was ethmoid followed by maxillary sinus. Bilateral disease was more common. Mucosal thickening with T2 hypointense septations was seen in 88.4% MRI studies. Periantral and orbital involvement was seen, respectively, in 84.6% and 55.7% cases of MRI. Intracranial involvement was noted in form of meningitis, cerebritis, abscess, infarct, hemorrhage, cavernous sinus, or perineural invasion. Vascular involvement was noted in form of vascular occlusion ($n = 3$), vascular narrowing ($n = 3$), and pseudoaneurysm ($n = 2$). MRI was more sensitive in detecting periantral

Keywords
- acute invasive fungal rhinosinusitis
- post-COVID-19
- COVID-19

article published online
April 14, 2023

DOI https://doi.org/10.1055/s-0043-1764351.
ISSN 2277-954X.

Thieme Medical and Scientific Publishers Pvt. Ltd., A-12, 2nd Floor, Sector 2, Noida-201301 UP, India

invasion, deep infratemporal fossa, cavernous sinus involvement, perineural invasion, optic nerve involvement, and vascular occlusion and narrowing, while CT was superior in identification of bony erosions.

Conclusion Early recognition of AIFR in post-COVID-19 patients is important to prevent disease-related morbidity/mortality. Several rarely described findings are noted in our series of AIFR, like optic nerve involvement, pituitary fungal abscess, perineural spread, fungal aneurysms, and arteritis-related posterior circulation infarcts. MRI is superior for early detection of disease and in estimation of extent of disease, compared with CT. Imaging can help in early detection of AIFR, which has a significant impact on patient outcome.

Background

Acute invasive fungal rhinosinusitis (AIFR) is a rare, rapidly progressive, and life-threatening infection involving the nasal cavity and paranasal sinuses.[1,2] The most predominant causative agents include *Aspergillus* and *Mucor* fungal species.[3] There was dramatic rise in AIFR cases in India, mostly seen in recently recovered or recovering coronavirus disease-2019 (COVID-19) patients.[4–9] India witnessed a dramatic spurt in cases of COVID-19-associated mucormycosis and by June 7, 2021, ~28,252 cases of mucormycosis were reported, with 86% of them having a history of COVID-19 infection.[10,11] Although the exact cause of this surge is not clear, uncontrolled diabetes mellitus coexisting with coronavirus infection, prolonged or high-dose steroid therapy, and oxygen and ventilator support may have some role in triggering this fungal infection.[12]

Early identification of disease, initiation of antifungal drugs, and early surgical debridement are the mainstay of management. Although tissue diagnosis is mandatory for confirming diagnosis of AIFR, aggressive treatment has to be started based on clinical and radiological findings. Imaging helps in early diagnosis as well as evaluation of extent of disease and hence plays a vital role in starting timely intervention. However, early imaging markers are not well known. Also, there is overlap between imaging features of sinusitis due to fungal etiology versus other infective etiology. Malignant lesions of paranasal sinuses also need to be differentiated from invasive infective etiology.

Few studies have described imaging features of COVID-19-associated AIFR.[10,13–19] We have described imaging findings in 90 studies including computed tomography (CT) and magnetic resonance imaging (MRI) of 60 patients of post-COVID-19 AIFR admitted and managed at our institute.

Methods

This was a retrospective review approved by the institutional review board conducted between May and July 2021. We reviewed imaging findings in post-COVID-19 patients who were admitted at our hospital with rhinosinusitis. Inclusion criteria were: (1) post-COVID-19 patients with rhinosinusitis who had proven fungal etiology on potassium hydroxide smear or histopathology; (2) clinical course less than 4 weeks; and (3) MRI and/or CT of craniofacial region done within 5 days before surgery. Patients without history of COVID-19 infection were excluded. Epidemiological and clinical data including age, sex, diabetes status, and history of oxygen therapy or steroid therapy were noted.

Noncontrast CT was done on 128-detector row multidetector CT scanner (GE Healthcare, Milwaukee, Wisconsin, United States) using 150 to 170 mm field of view and was acquired as 1-mm thick sections in axial plane. Reconstruction was done in coronal and sagittal planes. Soft tissue and bone algorithm were used.

MRI was done using 1.5-T MRI machine (GE Healthcare, Milwaukee, Wisconsin, United States). Routine sequences of brain (T1-weighted image, T2-weighted image, fluid attenuated inversion recovery, diffusion-weighted imaging, gradient echo with/without postcontrast ultrafast spoiled gradient echo 3D [brain volume imaging] sequence along with sinus and orbit sequences [2-mm thin sections including axial T2 fat-saturated, T1-weighted, postcontrast T1 Fast Spin Echo (FSE) fat-saturated images; 2-mm thin coronal sections including T2 fat-saturated, postcontrast T1 FSE fat-saturated images]) were obtained. Same protocol was followed in all patients. Additionally, Constructive Interference in Steady State (CISS) 3D was done when perineural spread was suspected based on above given sequences.

Site of involvement, unilateral/bilateral involvement, pattern of mucosal thickening, periantral invasion, orbital invasion, enhancement pattern, intracranial involvement, perineural spread, vascular involvement, and bony involvement were recorded.

Periantral fat invasion or orbital invasion was diagnosed by assessing pre- and postmaxillary fat space or orbits for evidence of soft tissue on T1-weighted axial images. The same structures were evaluated for presence of edema on T2-weighted fat-suppressed axial/coronal MRI sequences or for abnormal enhancement on postcontrast T1 FSE fat-saturated axial/coronal sequences.

Enhancement pattern of mucosal thickening and nasal cavity/paranasal sinus contents was assessed as presence or absence of focal areas of lack of contrast enhancement (LOCE).

Perineural spread was identified in forms of thickening (on MRI/CT) and enhancement (on MRI) along involved cranial nerve.

Patients with vascular involvement in form of fungal aneurysms were further evaluated using CT angiography and cerebral digital subtraction angiography.

We also studied involvement of structures on basis of seven imaging features of previously described CT model (periantral fat, bone dehiscence, orbital invasion, septal ulceration, pterygopalatine fossa, nasolacrimal duct, and lacrimal sac).

Comparison between MRI and CT features was done for patients who underwent CT and MRI imaging on the same day. Ability to detect periantral invasion, orbital invasion, infratemporal fossa invasion, cavernous sinus involvement, perineural spread, and optic nerve involvement was compared between the two modalities.

Results

We analyzed findings in 90 studies (CT and MRI) in 60 patients. Age ranged from 26 to 74 years (mean age 51 years) with 55 male and 15 female patients. Overall, 95% (57/60) patients had diabetes, 88.3% (53/60) patients received oxygen therapy, and 65% (39/60) patients received steroid therapy. There were 30 patients who underwent both CT and MRI study at the same time. Twenty-two patients had only MRI study available and eight patients had only CT study available. The findings are described below.

MRI Study

Fifty-two MRI studies (in 49 males and 13 females) were analyzed. Mucosal thickening and secretions were found to have mixed signal intensity on T2-weighted image with areas of T2 hyperintensity and foci of hypointensity. Site of involvement in nasal cavity and paranasal sinuses is described in ►**Table 1**. MRI findings are shown in ►**Fig. 1**.

Among 51 cases of maxillary sinus mucosal thickening, there was pattern of mucosal thickening with T2 hypointense septations identified in 46 cases and smooth mucosal thickening identified in 5 cases. Mucosal thickening with T2 hypointense septations was characterized by undulated surface of mucosal thickening with presence of septations and foci of T2 hypointensity (►**Fig. 1**). This pattern was partially/completely filling the sinus (►**Fig. 1A** and **E**). Air fluid level was noted in 5/52 (9.6%) cases on MRI.

Number of cases showing orbital and periantral invasion is described in ►**Table 1**. Contrast-enhanced sequences were available in 40 cases. Enhancement without focal areas of LOCE (LOCE –ve) was noted in 12 (30%) cases and enhancement with focal areas of LOCE (LOCE +ve) was noted in 28 cases (70%), shown in ►**Fig. 1**. LOCE involving turbinates (Black turbinate sign) was noted in 17/40 cases (42.5%).

Orbital involvement in MRI is described in ►**Table 2** and shown in ►**Fig. 2**. Intracranial and vascular involvement is described in ►**Table 3** and shown in ►**Figs. 3** and **4**. One or a combination of more than one finding of focal areas of loss of contrast enhancement, periantral invasion, orbital invasion, intracranial invasion, and vascular involvement on MRI were noted in 50/52 cases (96.1%).

CT Study

Site of involvement in nasal cavity and paranasal sinuses, and periantral and orbital invasion are described in ►**Table 1**. Air fluid level was noted in 7/38 (18.4%) studies. Bony erosions were noted in 8/38 (21%) cases. Intracranial and vascular involvement is described in ►**Table 3**. Suspected cases of fungal aneurysms were evaluated using CT angiography ($n = 2$), which revealed aneurysm in two cases.

We also studied involvement of structures on basis of seven imaging features of previously described CT model (periantral fat, bone dehiscence, orbital invasion, septal ulceration, pterygopalatine fossa, nasolacrimal duct, and lacrimal sac). Two or more of these variables were involved in 29/38 (76.3%) cases. CT findings are shown in ►**Fig. 5**.

Comparison of CT and MRI

There were 30 patients who underwent both CT and MRI imaging on the same day. There was orbital fat infiltration noted in 20/30 (66.7%) cases in both MRI and CT studies.

Table 1 Involvement of structures on CT and MRI

Structures involved	Number of cases on CT ($n = 38$)	Number of cases on MRI ($n = 52$)
Nasal cavity	29: unilateral 16, bilateral 13	46: unilateral 20, bilateral 26
Ethmoid	37	52
Maxillary	36	51
Sphenoid	27	40
Frontal	28	37
Periantral invasion	26	44
Orbital invasion	24	29
Deep infratemporal fossa muscle plane invasion	4	37
Pterygopalatine fossa invasion	14	–

Abbreviations: CT, computed tomography; MRI, magnetic resonance imaging.

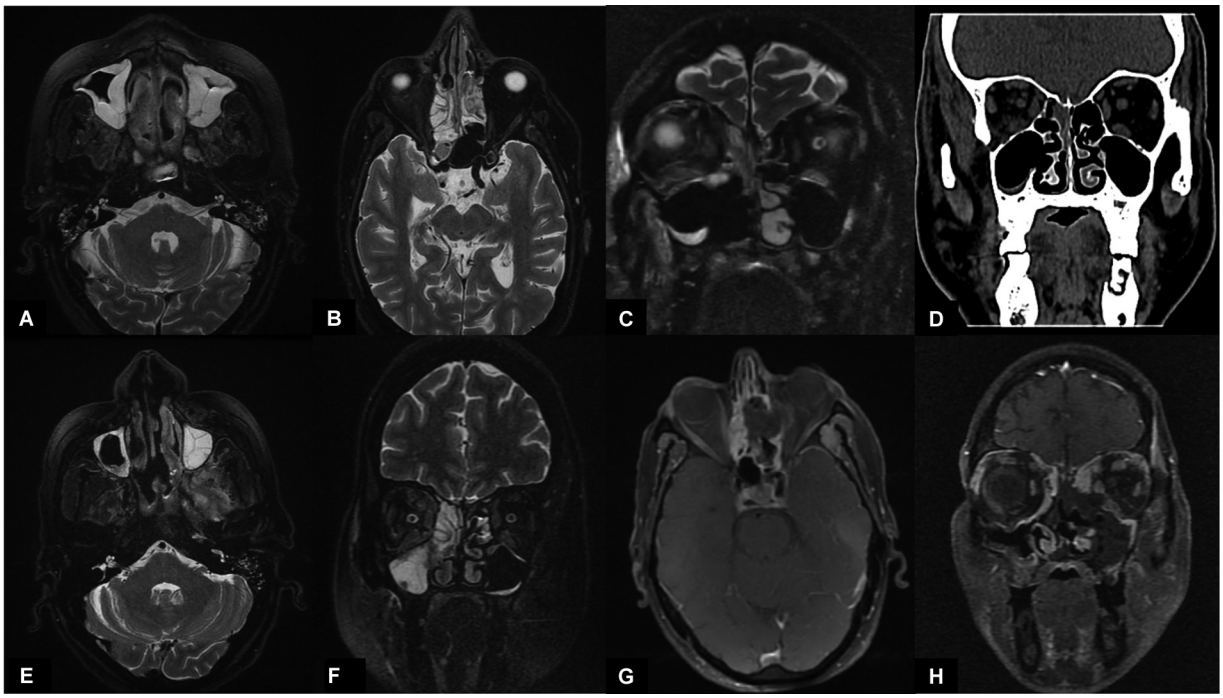

Fig. 1 Imaging features of acute invasive rhinosinusitis on magnetic resonance imaging. (**A**) T2-weighted axial image showing nodular mucosal thickening in left maxillary sinus with foci of T2 hypointensity. (**B**) T2-weighted axial image showing mucosal thickening in bilateral ethmoid sinuses with foci of T2 hypointense signal. (**c**) Coronal T2-weighted image shows complete T2 hypointense signal involving right middle and inferior turbinate with signal as black as surrounding air. (**D**) Computed tomography image: coronal cut of same patient as in (**C**) showing hyperdense right middle and inferior turbinate. (**E**) Axial T2-weighted fat-saturated image shows nodular mucosal thickening in bilateral maxillary sinus with periantral fat stranding, edema in left retroantral space, left infratemporal fossa, and left pterygopalatine fossa. (**F**) T2-weighted coronal image shows mucosal thickening in right ethmoid and right maxillary sinuses with fat stranding in right orbital fat. (**G**) Postcontrast fat-saturated T1-weighted axial image shows heterogeneous enhancement of mucosal thickening in bilateral ethmoid sinuses with focal areas of lack of contrast enhancement. (**H**) Postcontrast fat-saturated T1-weighted coronal image shows heterogeneous enhancement of mucosal thickening in bilateral ethmoid sinuses with focal areas of lack of contrast enhancement.

Periantral fat invasion was noted in 25/30 (83.3%) cases in MRI and in 22/30 (73.3%) cases in CT. CT could not identify periantral fat invasion in three cases, which were picked up on MRI. Deep infratemporal fossa involvement in form of edema/soft tissue was noted in 20/30 (66.7%) cases in MRI and in 4/30 (13.3%) cases in CT. CT could not identify deep infratemporal involvement in 16 cases, which was positively identified on MRI. MRI identified cavernous sinus involvement in form of bulkiness of cavernous sinus with T2 hypointense soft tissue in 7/30 (23.3%) cases and in form of thrombosis in 1/30 (3.3%) cases. CT identified soft tissue in 1/30 (3.3%) cases. Noncontrast CT was available, so cavernous sinus thrombosis could not be evaluated on CT. Perineural spread along trigeminal nerve was noted in 8/30 (26.7%) cases on MRI, while it could be identified only in 2/30 (6.7%) cases on CT studies. Similarly, optic nerve involvement, which was picked up on MRI on diffusion-weighted images (7/30, i.e., 23.3% studies), could not be identified on CT, which only showed perioptic fat stranding.

Table 2 Orbital involvement on MRI

Type of involvement	Number of cases on MRI ($n = 52$)
Fat invasion	29
Soft tissue	24
Peripherally enhancing collection	5
Optic nerve diffusion restriction	10
Endophthalmitis	1

Abbreviation: MRI, magnetic resonance imaging.

Discussion

Invasive fungal rhinosinusitis is a rare disease that has high mortality and morbidity. Early diagnosis and initiation of therapy is essential for proper management. Radiologic imaging features have been previously described. Previous studies had focused on presence of bony erosions (diagnosed on CT). However, these are late findings. Recent literature has focused on MRI and CT studies to diagnose early infiltrative signs and development of soft tissue abnormalities.

Most common site of involvement in our study was ethmoid sinus followed by maxillary sinus. Previously described most commonly involved sinuses are maxillary sinus, ethmoid air cells, and sphenoid sinus, with the frontal sinus being reported as the least frequently affected, which is similar to our results.[20,21]

Unilateral nasal cavity disease was noted in 38.4% of MRI and 42% of CT studies. Unilateral nasal cavity disease has been described as a common finding in invasive fungal

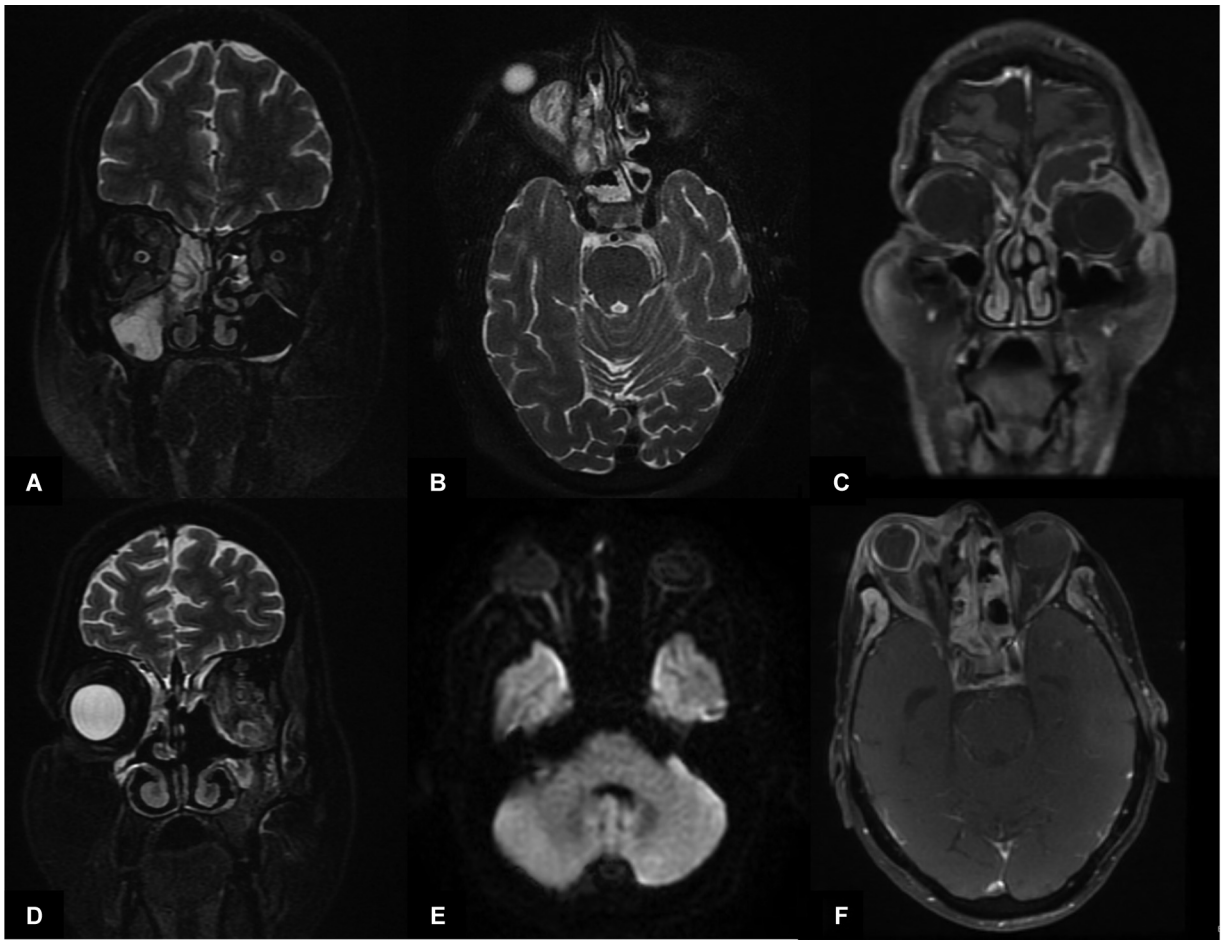

Fig. 2 Magnetic resonance imaging features of orbital involvement. (**A**) T2 Fat Saturated (FS) coronal image shows mucosal thickening and T2 hypointensity involving right maxillary and ethmoid sinuses with fat stranding involving right orbital fat. (**B**) Axial T2 FS image shows T2 heterogeneous soft tissue involving right orbit in continuity with T2 heterogeneous mucosal thickening involving right ethmoid sinus. (**C**) Postcontrast T1 FS coronal image shows peripherally enhancing collection involving left frontal sinus with continuous involvement of left superior extraconal portion of left orbit, suggestive of left frontal sinus and left orbital abscess. (**D**) T2 FS coronal image shows mucosal thickening involving bilateral ethmoid sinuses with T2 hypointense signal involving left middle turbinate. Left orbit shows fat stranding with bulky extraocular muscles and T2 hypointense thickened left optic nerve. (**E**) Diffusion-weighted imaging trace axial image shows diffusion restriction involving right optic nerve. (**F**) Postcontrast T1 FS axial image shows enhancing mucosal thickening involving bilateral ethmoids with focal area of lack of contrast enhancement in right ethmoid sinus. Ill-defined enhancement noted in right orbit with nonenhancing soft tissue. Enhancement of uvea noted involving right globe suggestive of endophthalmitis.

disease; however, it is not specific.[21,22] Although it is not commonly seen in viral or bacterial rhinosinusitis, yet, as a standalone finding, it is not a strong individual predictor of invasive fungal etiology.[21] Middlebrooks et al found that 78.6% of their patients had unilateral predominant findings, while bilateral involvement was more common in our series.[21] In a study by Slonimsky et al, they found that AIFR caused by *Mucor* species demonstrated a higher degree of bilateral sinonasal involvement as compared with *Aspergillus*, which had predominant unilateral involvement.[2] The same may be the reason for findings in our study. We did not study the difference between *Aspergillus* and *Mucor* species as we did not have histopathological information for all cases. In majority of cases, microscopy prohibits conclusive differentiation of *Mucorales* from *Aspergillus* and other filamentous fungi.[23,24]

We noted that mucosal thickening with T2 hypointense septations was noted in a high percentage of cases in MRI (88.4%) (►**Fig. 1**). Previously described studies have shown presence of nodular mucosal thickening as a feature of AIFR.[25–27] Another study described presence of smooth mucosal thickening in AIFR.[28] However, these studies have mostly described involvement in radiographs or CT and MRI pattern of mucosal thickening has not been clearly described. We propose that this pattern of mucosal thickening with T2 hypointense septations, if present, can help in diagnosis toward fungal etiology. Similar pattern of mucosal thickening can be seen in retention cysts or nasal polyps. Retention cysts are usually mostly located in dependent portion of sinuses without extension to nasal cavity, while this pattern of mucosal thickening with T2 hypointense septations usually uniformly involves the sinus mucosa. Polyps can have similar imaging appearance and usually extend into nasal cavity. Most importantly, we noted that evidence of perisinus invasion with associated septations of mucosal thickening should alert toward fungal etiology.

Table 3 Intracranial and vascular involvement on CT and MRI

Intracranial structure involvement	Number of cases on CT ($n = 38$)	Number of cases on MRI ($n = 52$)
Cavernous sinus thrombosis	–	2
Cavernous sinus soft tissue	3	15
Meningitis	–	8 (4 had leptomeningitis and 4 had pachymeningitis
Cerebritis	8	7
Abscess	–	2
Perineural invasion	3	8
Infarct	6 (2 in MCA territory, 3 in watershed zones, and 1 in MCA and AICA territories each)	9 (3 in MCA territory, 5 in watershed zones, and 1 in MCA and AICA territories each)
Vascular occlusion	–	3 (ICA occlusion)
Vascular narrowing	–	3 (ICA narrowing)
Aneurysm	2	–
Hemorrhage	2 (parenchymal bleed along with sylvian SAH in one case and basilar cistern SAH in second case)	–

Abbreviations: AICA, Anterior Inferior Cerebellar Artery; CT, computed tomography; ICA; internal carotid artery; MCA, Middle cerebral artery; MRI, magnetic resonance imaging; SAH, Subarachnoid Hemorrhage.

Additionally, there is absence of additional areas of T2 hypointensity, and absence of focal areas of LOCE in nasal polyposis/retention cysts. These features may help to differentiate it from fungal-etiology-associated T2 hypointense septations.

Air fluid levels are uncommon in AIFR and is a more common finding noted in bacterial rhinosinusitis.[22,25,26,28,29] Similar findings were noted in our study whereby air fluid level was noted in 9.6% cases on MRI and 18.4% cases on CT and involving total 8/60 patients (13.3%).

Periantral fat involvement was noted in 68.4% cases of CT and in 84.6% cases of MRI. Infiltration of periantral fat has been described as an early indicator of AIFR.[30] In a study of CT findings of AIFR, it was described as the best individual predictor; however, by itself, it had a sensitivity of only 74%, which is comparable to our findings.[21] A recent study has described perisinus inflammation in 100% of their cases.[15]

We noted that areas of LOCE were noted in sinonasal tract and extrasinus location in 28/40 (70%) cases (40 contrast-enhanced MRI scans were available) (►**Fig. 1**). These areas of LOCE have been previously described[31–34] and were reported in 74% cases of invasive fungal sinusitis, which is comparable to our study. Angioinvasive nature leads to tissue infarction, which has been proposed to be the cause for this pattern of focal areas of LOCE.

We found diffusion restriction involving optic nerves in 10 cases (►**Fig. 2**). Optic nerve diffusion restriction in fungal rhinosinusitis was previously described in a few case reports.[35–38] Recent series by Kumar et al described ischemic optic neuropathy in 12 cases.[15] Another series by Elmokadem et al described optic neuritis (T2 hyperintensity of optic nerves) in six cases.[16] We describe cases with diffusion restriction involving optic nerve due to fungal rhinosinusitis. Interestingly, all these cases with optic nerve diffusion restriction had fat infiltration and soft tissue involving orbital apex. Orbital apex involvement with soft tissue may cause central retinal artery occlusion, ophthalmic artery necrosis, optic nerve infarction and necrosis, or direct optic nerve infection by mucormycosis.[35,39,40]

Bone erosion was noted in 21% of CT studies. It is described as a late feature and is not very sensitive.[2] Bony dehiscence was reported to have 100% specificity and 35% sensitivity for AIFR.[21] Elmokadem described bony involvement in 64% of their cases.[16] It is not necessarily present in all cases of AIFR that show invasion. This is because of spread of fungal elements along vascular channels in bone.

We noted intracranial involvement in form of meningitis, fungal cerebritis, fungal abscess, cavernous sinus thrombosis/soft tissue, perineural invasion, parenchymal infarcts, and parenchymal/subarachnoid hemorrhage. We noted a case of pituitary fungal abscess due to contiguous spread from sphenoid sinus (►**Fig. 3**). Fungal abscess of pituitary has been described in fewer than 10 case reports.[41–49]

Perineural spread along trigeminal nerve was seen in 8/52 (15.4%) cases (►**Fig. 3**). Perineural spread in AIFR is also a rare finding, previously described only in a few case reports.[38,50–53] In a recently described series of cases of COVID-19-associated rhino-orbito-cerebral mucormycosis by Kumar et al,[15] perineural spread was described in 29 cases (28.7%). Most commonly, involvement of trigeminal or olfactory nerves has been described.

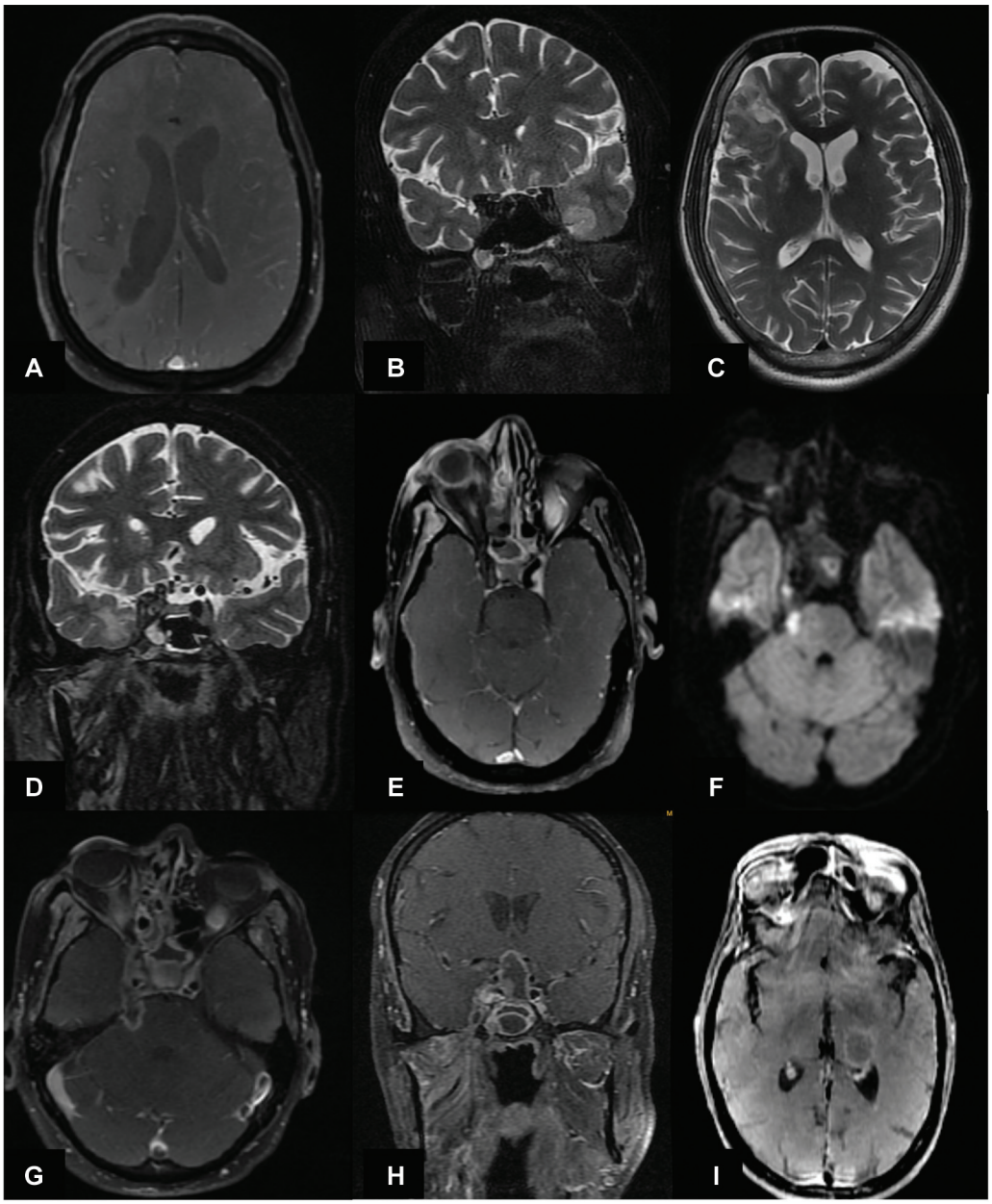

Fig. 3 Intracranial involvement in acute invasive fungal rhinosinusitis. (**A**) Postcontrast T1 axial image shows diffuse leptomeningeal and pachymeningeal enhancement suggestive of meningitis. (**B**) Coronal and (**C**) axial T2-weighted images show T2 hyperintense signal in cortical-subcortical location involving left temporal lobe and right frontal lobe, respectively, suggestive of cerebritis. (**D**) Coronal T2-weighted image shows T2 hypointense soft tissue involving right cavernous sinus with loss of flow void of right internal carotid artery. (**E**) Axial postcontrast T1 FS image shows enhancing mucosal thickening with areas of loss of enhancement involving right ethmoid sinus with nonenhancement of right cavernous sinus suggestive of cavernous sinus thrombosis. Ill-defined enhancement is noted in right orbit with associated right globe uveal enhancement suggestive of endophthalmitis. (**F**) Axial diffusion-weighted imaging trace image shows diffusion restriction involving cisternal segment of right trigeminal nerve. (G) Postcontrast T1 axial image of same patient as in (**F**) shows peripheral enhancement and thickening involving right trigeminal nerve cisternal segment suggestive of perineural spread. (**H**) Postcontrast T1 FS coronal image shows peripherally enhancing collection involving sphenoid sinus with contiguous involvement of sella and suprasellar space suggestive of pituitary abscess. Associated involvement of right cavernous sinus also noted. (**I**) Postcontrast T1 image showing peripherally enhancing lesion involving left thalamus. The lesion showed diffusion restriction (not shown). Features suggestive of left thalamic abscess (hematogenous spread).

We also noted two cases of internal carotid artery (ICA) fungal aneurysms, one involving supraclinoid ICA (ruptured) and another involving cavernous ICA (unruptured) (►**Fig. 4**). Fungal aneurysms are very rare and less than 25 cases have been described.[14,15,54–56] They show hyphal growth along the vessel wall resulting from direct spread or through hematogenous spreading, and characteristic fusiform shape has been described similar to our cases. Intradural ICA is most commonly described location of these aneurysms, which was noted in one of our cases.

Two of our patients had cavernous sinus involvement with MCA territory infarct with perineural spread along trigeminal nerve and ipsilateral AICA territory infarct (one case shown in ►**Fig. 4**). This interesting pattern of

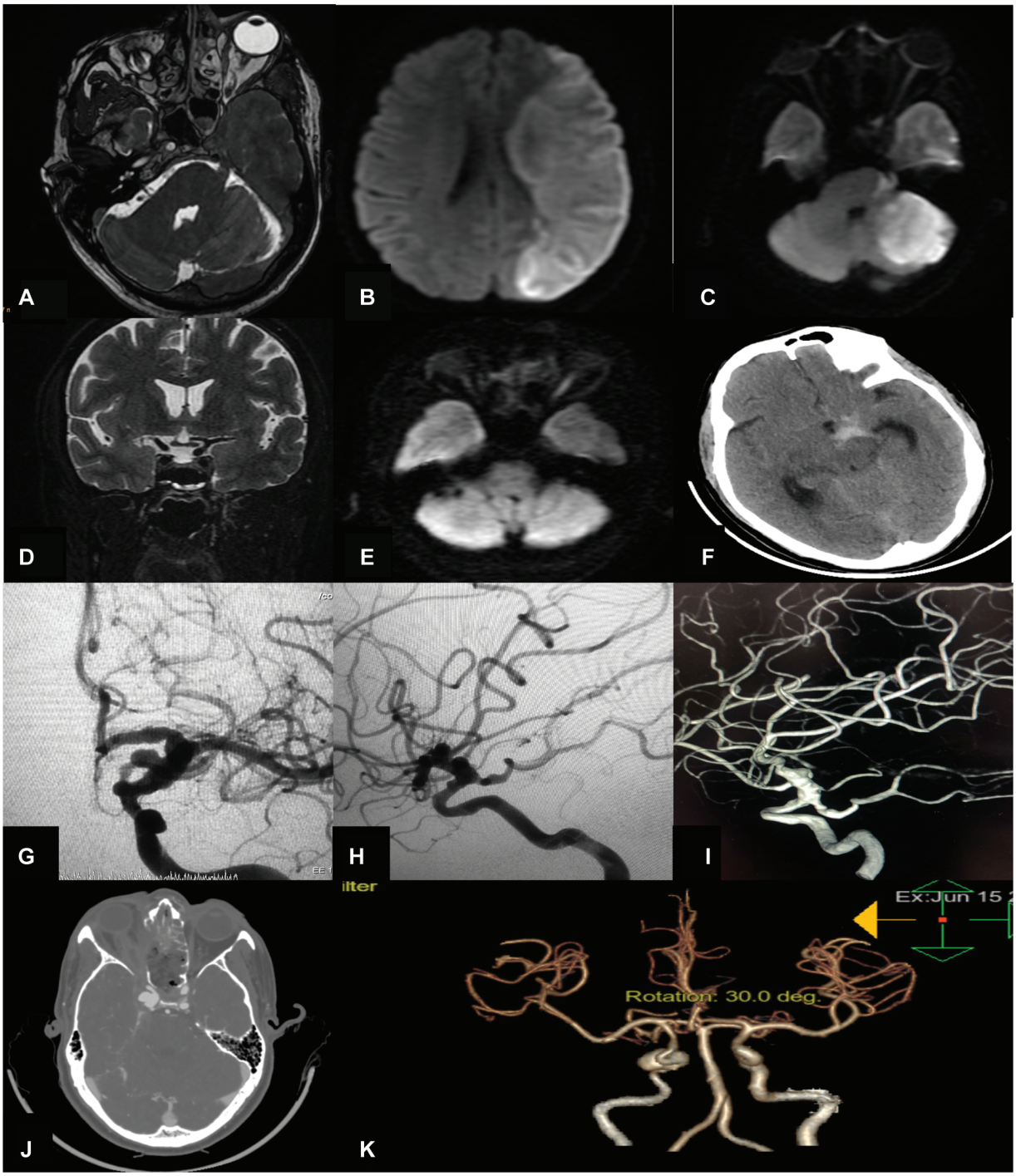

Fig. 4 Vascular involvement in acute invasive fungal rhinosinusitis. (**A**) CISS 3D axial image showing mucosal thickening with foci of T2 hypointense signal noted in bilateral ethmoid and left side of sphenoid sinus with T2 hypointense signal involving left cavernous sinus with loss of signal of left internal carotid artery (ICA). (**B**) Diffusion-weighted imaging (DWI) trace axial image shows left MCA territory infarct. (**C**) DWI trace axial image in lower section shows diffusion restriction along left trigeminal nerve with left AICA territory infarct (likely due to arteritis involving left AICA, which was noted in close relation to left trigeminal nerve with perineural spread). (**D**) Coronal T2-weighted image showing bulky T2 hypointense left cavernous sinus with normal appearance of left terminal ICA. (**e**) Same patient DWI axial image shows diffusion restriction involving left optic nerve. (**F**) Computed tomography (CT) scan of same patient as in (**D, E**) done after 7 days due to new development of severe headache and sensorium shows SAH involving left side of basal cistern and left crural cistern. (**G**) Cerebral angiography anteroposterior image of the same patient as in (**D, E, F**) shows fusiform dilatation of left supraclinoid and terminal ICA with saccular aneurysm in left supraclinoid segment, which developed within an interval of 7 days and was not noted in previous magnetic resonance imaging (in **D**). (**H, I**) Lateral angiogram and 3D image showing the aneurysm. (**J**) Different patient axial CT angiography image showing bilateral ethmoid sinus mucosal thickening with right lamina papyracea erosion with right cavernous ICA aneurysm. (**K**) VRT image of same patient as in (**J**) showing fungal aneurysm involving right cavernous ICA.

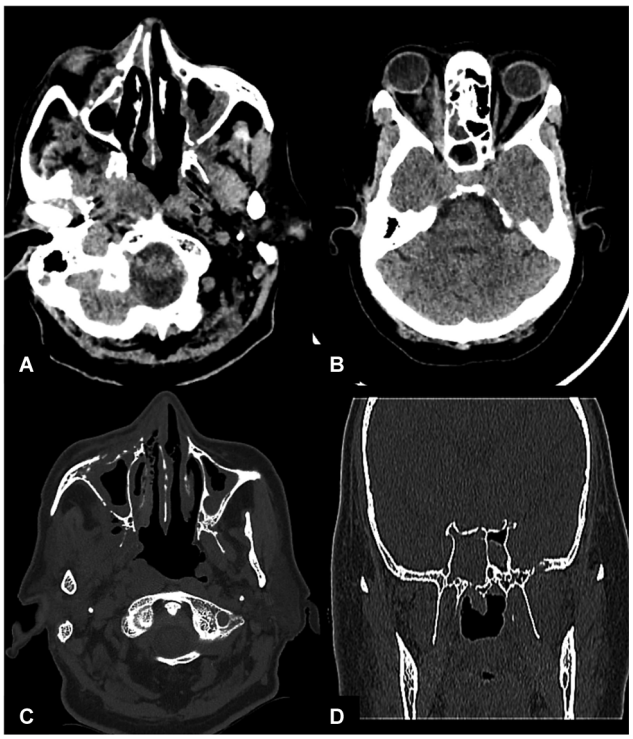

Fig. 5 Imaging features of acute invasive rhinosinusitis on computed tomography (CT). (**A**) Axial CT shows nodular mucosal thickening in left maxillary sinus with soft tissue in left retroantral space and left pterygopalatine fossa. (**B**) Axial CT shows mucosal thickening in right ethmoid sinuses with right orbital proptosis and isodense soft tissue in right orbit involving medial extraconal space and intraconal space with associated right orbital fat stranding. (**C**) Bone window axial section shows erosions involving right maxillary sinus anterior and posterolateral walls as well as erosion of right pterygoid plates. Periantral soft tissue noted on right side. (**D**) Bone window coronal section shows mucosal thickening in sphenoid sinus and erosions involving left middle cranial fossa floor.

involvement can be explained by involvement of cavernous sinus, leading to ICA wall inflammation that can cause infarct in MCA territory. Additionally, perineural spread along trigeminal nerve can cause arteritis of adjacent AICA, leading to ipsilateral AICA territory infarct. Basilar arteritis leading to pontine infarction due to intracranial mucormycosis has been described.[57] Vasculitis due to fungal etiology most commonly occurs in the supraclinoid portion of the ICA, and posterior circulation vessel involvement is rare and usually occurs late.

In a previous study, Middlebrooks et al[21] described seven variable CT models (periantral fat, bone dehiscence, orbital invasion, septal ulceration, pterygopalatine fossa, nasolacrimal duct, and lacrimal sac) that were noted to be easily applicable and robust screening tools to detect AIFR. It was noted that presence of any two variables predicted AIFR with 100% specificity, 100% positive predictive value, and 88.1% sensitivity. We noted that 2 or more of these 7 variables were involved in 29/38 cases, with a sensitivity of 76.3%, which is slightly lower than that described by Middlebrooks et al. This may be due to imaging early, in the course of disease, the patients in our study. However, our study reinforces the importance of utilization of these seven variable models on CT that can help in early identification of AIFR.

We studied a combination of findings on MRI including focal areas of loss of contrast enhancement, periantral invasion, orbital invasion, intracranial invasion, and vascular involvement. One or more of these findings were noted in 50/52 cases (96.1%). The two cases that had neither of these findings were noted to have mucosal thickening, with T2 hypointense septations in both cases. Patients with early disease may not show either of these five described features; in such patients, presence of mucosal thickening with T2 hypointense septations in sinuses/nasal cavity should alert toward possibility of fungal etiology and close follow-up of these patients should be done.

We found that on comparison of CT and MRI performed simultaneously, both CT and MRI had equal sensitivity in diagnosis of orbital fat invasion while MRI was more sensitive in diagnosis of periantral fat invasion. Similar to our findings, MRI was noted to have a higher sensitivity (87–100%) as compared with CT (57–87%) in detection of extrasinus invasion.[58] We also noted that deep infratemporal fossa involvement in forms of edema/soft tissue, cavernous sinus involvement, and perineural invasion was also identified with higher sensitivity on MRI as compared with CT. Optic nerve involvement could only be identified on MRI. Even without angiography, MRI was able to identify vascular occlusion and narrowing in cavernous ICA. Even though CT is superior in identification of bony erosions, bony involvement is seen late in the disease process and noted in relatively low percentage of cases. Thus, MRI should be the preferred imaging modality for early detection of AIFR as well as for accurate estimation of the extent of the disease.

Our study has few limitations. We did not have a control group and did not compare imaging findings of AIFR with other nonfungal etiologies of sinus pathologies like bacterial sinusitis, benign polyps, allergic sinusitis, and neoplastic etiologies. We also did not evaluate features to differentiate between various fungal species. There was also lack of histopathological correlate of imaging features such as T2 hypointense septations, optic nerve diffusion restriction, areas of LOCE, and perineural spread. These may form a part of future thrust areas and future studies.

Conclusion

Various CT and MRI features to help in early recognition of AIFR in post-COVID-19 patients have been described. Several rarely described findings are noted in our series of AIFR like optic nerve involvement, pituitary fungal abscess, perineural spread, fungal aneurysms, and arteritis-related posterior circulation infarcts. MRI is superior for early detection of disease and in estimation of extent of disease, compared with CT. Imaging can help in early detection of AIFR, which has a significant impact on patient outcome.

Ethical Approval Statement

The study has been approved by the appropriate ethics committee.

Consent for Publication

Written consent to publish information was obtained from study participants. Informed consent was gathered from the patient and consent to publish images was obtained.

Data Availability Statement

The datasets used and/or analyzed during the current study can be provided by the corresponding author on reasonable request.

Authors' Contribution

N.Y. was involved in literature search, figures, data collection, data analysis, data interpretation, and writing. A.K. contributed to literature search, revision, and editing of manuscript. K.S. and S.A. were involved in data collection, revision, and editing of manuscript. All authors read and approved the final manuscript.

Conflict of Interest

None declared.

References

1 Aribandi M, McCoy VA, Bazan C III. Imaging features of invasive and noninvasive fungal sinusitis: a review. Radiographics 2007; 27(05):1283–1296

2 Slonimsky G, McGinn JD, Goyal N, et al. A model for classification of invasive fungal rhinosinusitis by computed tomography. Sci Rep 2020;10(01):12591

3 Parikh SL, Venkatraman G, DelGaudio JM. Invasive fungal sinusitis: a 15-year review from a single institution. Am J Rhinol 2004;18(02): 75–81

4 Sarkar S, Gokhale T, Choudhury SS, Deb AK. COVID-19 and orbital mucormycosis. Indian J Ophthalmol 2021;69(04): 1002–1004

5 Mehta S, Pandey A. Rhino-Orbital Mucormycosis Associated With COVID-19. Cureus [Internet]. Accessed Feb 7, 2023, at: https://www.ncbi.nlm.nih.gov/pmc/articles/PMC7599039/

6 Mishra N, Mutya VSS, Thomas A, et al. A case series of invasive mucormycosis in patients with COVID-19 infection. Int J Otorhinolaryngol Head Neck Surg 2021;7(05):867–870

7 Maini A, Tomar G, Khanna D, Kini Y, Mehta H, Bhagyasree V. Sino-orbital mucormycosis in a COVID-19 patient: a case report. Int J Surg Case Rep 2021;82:105957

8 Saldanha M, Reddy R, Vincent MJ. Title of the article: paranasal mucormycosis in COVID-19 patient. Indian J Otolaryngol Head Neck Surg 2022;74:3407–3410

9 Nehara HR, Puri I, Singhal V, Ih S, Bishnoi BR, Sirohi P. Rhinocerebral mucormycosis in COVID-19 patient with diabetes a deadly trio: case series from the north-western part of India. Indian J Med Microbiol [Internet]. 2021 Accessed Feb 7, 2023, at: https://www.sciencedirect.com/science/article/pii/S0255085721041116

10 Khullar T, Kumar J, Sindhu D, Garg A, Meher R. CT imaging features in acute invasive fungal rhinosinusitis- recalling the oblivion in the COVID era. Curr Probl Diagn Radiol 2022;51(05):798–805

11 Arora R, Goel R, Khanam S, et al. Rhino-orbito-cerebral-mucormycosis during the COVID-19 second wave in 2021 - a preliminary report from a single hospital. Clin Ophthalmol 2021; 15:3505–3514

12 Song G, Liang G, Liu W. Fungal co-infections associated with global COVID-19 pandemic: a clinical and diagnostic perspective from China. Mycopathologia 2020;185(04):599–606

13 Sweed AH, Mobashir M, Elnashar I, et al. MRI as a road map for surgical intervention of acute invasive fungal sinusitis in Covid-19 era. Clin Otolaryngol 2022;47(02):388–392

14 Ashour MM, Abdelaziz TT, Ashour DM, Askoura A, Saleh MI, Mahmoud MS. Imaging spectrum of acute invasive fungal rhino-orbital-cerebral sinusitis in COVID-19 patients: a case series and a review of literature. J Neuroradiol 2021;48(05):319–324

15 Kumar Gg S, Deepalam S, Siddiqui A, et al. Coronavirus Disease 2019 (COVID-19)-associated rhino-orbito-cerebral mucormycosis: a multi-institutional retrospective study of imaging patterns. World Neurosurg 2022;162:e131–e140

16 Elmokadem AH, Bayoumi D, Mansour M, Ghonim M, Saad EA, Khedr D. COVID-19-associated acute invasive fungal sinusitis: clinical and imaging findings. J Neuroimaging 2022;32(04): 676–689

17 Khullar T, Kumar J, Sindhu D, Garg A, Meher R, Goel R. Coronavirus disease 2019 associated mucormycosis meandering its way into the orbit: a pictorial review. J Laryngol Otol 2021;135(11): 942–946

18 Agarwal S, Gautam R, Kumar J, et al. COVID-associated sinonasal mucormycosis: radiological pathological correlation and prognostic value of MR imaging. Indian J Radiol Imaging [Internet] 2022;33(01):46–52

19 Sehgal A, Kumar J, Garg A, et al. MR imaging spectrum in COVID associated rhino-orbito-cerebral mucormycosis with special emphasis on intracranial disease and impact on patient prognosis. Eur J Radiol 2022;152:110341

20 Gillespie MB, O'Malley BW Jr, Francis HW. An approach to fulminant invasive fungal rhinosinusitis in the immunocompromised host. Arch Otolaryngol Head Neck Surg 1998;124(05):520–526

21 Middlebrooks EH, Frost CJ, De Jesus RO, Massini TC, Schmalfuss IM, Mancuso AA. Acute invasive fungal rhinosinusitis: a comprehensive update of CT findings and design of an effective diagnostic imaging model. AJNR Am J Neuroradiol 2015;36(08): 1529–1535

22 DelGaudio JM, Swain RE Jr, Kingdom TT, Muller S, Hudgins PA. Computed tomographic findings in patients with invasive fungal sinusitis. Arch Otolaryngol Head Neck Surg 2003;129(02): 236–240

23 Lackner N, Posch W, Lass-Flörl C. Microbiological and molecular diagnosis of mucormycosis: from old to new. Microorganisms 2021;9(07):1518

24 Lass-Flörl C, Samardzic E, Knoll M. Serology anno 2021-fungal infections: from invasive to chronic. Clin Microbiol Infect 2021;27 (09):1230–1241

25 Chan LL, Singh S, Jones D, Diaz EM Jr, Ginsberg LE. Imaging of mucormycosis skull base osteomyelitis. AJNR Am J Neuroradiol 2000;21(05):828–831

26 Centeno RS, Bentson JR, Mancuso AA. CT scanning in rhinocerebral mucormycosis and aspergillosis. Radiology 1981; 140(02):383–389

27 Green WH, Goldberg HI, Wohl GT. Mucormycosis infection of the craniofacial structures. Am J Roentgenol Radium Ther Nucl Med 1967;101(04):802–806

28 Addlestone RB, Baylin GJ. Rhinocerebral mucormycosis. Radiology 1975;115(01):113–117

29 Gamba JL, Woodruff WW, Djang WT, Yeates AE. Craniofacial mucormycosis: assessment with CT. Radiology 1986;160(01): 207–212

30 Silverman CS, Mancuso AA. Periantral soft-tissue infiltration and its relevance to the early detection of invasive fungal sinusitis: CT and MR findings. AJNR Am J Neuroradiol 1998;19 (02):321–325

31 Horger M, Hebart H, Schimmel H, et al. Disseminated mucormycosis in haematological patients: CT and MRI findings with pathological correlation. Br J Radiol 2006;79(945):e88–e95

32 Choi YR, Kim JH, Min HS, et al. Acute invasive fungal rhinosinusitis: MR imaging features and their impact on prognosis. Neuroradiology 2018;60(07):715–723

33 Seo J, Kim HJ, Chung SK, et al. Cervicofacial tissue infarction in patients with acute invasive fungal sinusitis: prevalence and characteristic MR imaging findings. Neuroradiology 2013;55 (04):467–473

34 Safder S, Carpenter JS, Roberts TD, Bailey N. The "Black Turbinate" sign: an early MR imaging finding of nasal mucormycosis. AJNR Am J Neuroradiol 2010;31(04):771–774

35 Mathur S, Karimi A, Mafee MF. Acute optic nerve infarction demonstrated by diffusion-weighted imaging in a case of rhinocerebral mucormycosis. AJNR Am J Neuroradiol 2007;28 (03):489–490

36 Ghabrial R, Ananda A, van Hal SJ, et al. Invasive fungal sinusitis presenting as acute posterior ischemic optic neuropathy. Neuroophthalmology 2017;42(04):209–214

37 Alsuhaibani AH, Al-Thubaiti G, Al Badr FB. Optic nerve thickening and infarction as the first evidence of orbital involvement with mucormycosis. Middle East Afr J Ophthalmol 2012;19(03): 340–342

38 Ghuman MS, Kaur S, Bhandal SK, Ahluwalia A, Saggar K. Bilateral optic nerve infarction in rhino-cerebral mucormycosis: a rare magnetic resonance imaging finding. J Neurosci Rural Pract 2015; 6(03):403–404

39 Ferry AP, Abedi S. Diagnosis and management of rhino-orbitocerebral mucormycosis (phycomycosis). A report of 16 personally observed cases. Ophthalmology 1983;90(09):1096–1104

40 Downie JA, Francis IC, Arnold JJ, Bott LM, Kos S. Sudden blindness and total ophthalmoplegia in mucormycosis. A clinicopathological correlation. J Clin Neuroophthalmol 1993;13(01):27–34

41 Fuchs HA, Evans RM, Gregg CR. Invasive aspergillosis of the sphenoid sinus manifested as a pituitary tumor. South Med J 1985;78(11):1365–1367

42 Ramos-Gabatin A, Jordan RM. Primary pituitary aspergillosis responding to transsphenoidal surgery and combined therapy with amphotericin-B and 5-fluorocytosine: case report. J Neurosurg 1981;54(06):839–841

43 Larrañaga J, Fandiño J, Gomez-Bueno J, Rodriguez D, Gonzalez-Carrero J, Botana C. Aspergillosis of the sphenoid sinus simulating a pituitary tumor. Neuroradiology 1989;31(04):362–363

44 Parker KM, Nicholson JK, Cezayirli RC, Biggs PJ. Aspergillosis of the sphenoid sinus: presentation as a pituitary mass and postoperative gallium-67 imaging. Surg Neurol 1996;45(04): 354–358

45 Hao L, Jing C, Bowen C, Min H, Chao Y. Aspergillus sellar abscess: case report and review of the literature. Neurol India 2008;56 (02):186–188

46 Heary RF, Maniker AH, Wolansky LJ. Candidal pituitary abscess: case report. Neurosurgery 1995;36(05):1009–1012, discussion 1012–1013

47 Iplikcioglu AC, Bek S, Bikmaz K, Ceylan D, Gökduman CA. Aspergillus pituitary abscess. Acta Neurochir (Wien) 2004;146 (05):521–524

48 Liu J, You C, Tang J, Chen L. Fungal pituitary abscess: case report and review of the literature. Neurol India 2013;61(02): 210–212

49 Lee JH, Park YS, Kim KM, et al. Pituitary aspergillosis mimicking pituitary tumor. AJR Am J Roentgenol 2000;175(06):1570–1572

50 Maheshwari S, Patil M, Shendey S. Mucormycosis creeping along the nerves in an immunocompetent individual. J Radiol Case Rep 2019;13(10):1–10

51 McLean FM, Ginsberg LE, Stanton CA. Perineural spread of rhinocerebral mucormycosis. AJNR Am J Neuroradiol 1996;17 (01):114–116

52 Orguc S, Yücetürk AV, Demir MA, Goktan C. Rhinocerebral mucormycosis: perineural spread via the trigeminal nerve. J Clin Neurosci 2005;12(04):484–486

53 Sandron J, Hantson P, Duprez T. Intracranial brain parenchymal spread of mucormycosis through olfactory tract: a diffusion-weighted imaging-based concept. Acta Radiol Open 2020;9(12): 2058460120980999

54 Hurst RW, Judkins A, Bolger W, Chu A, Loevner LA. Mycotic aneurysm and cerebral infarction resulting from fungal sinusitis: imaging and pathologic correlation. AJNR Am J Neuroradiol 2001;22(05):858–863

55 Yamaguchi J, Kawabata T, Motomura A, Hatano N, Seki Y. Fungal internal carotid artery aneurysm treated by trapping and high-flow bypass: a case report and literature review. Neurol Med Chir (Tokyo) 2016;56(02):89–94

56 Tambuzzi S, Boracchi M, Maciocco F, Tonello C, Gentile G, Zoja R. Fungal aneurism of the right posterior inferior cerebellar artery (PICA). Med Mycol Case Rep 2019;26:25–27

57 Calli C, Savas R, Parildar M, Pekindil G, Alper H, Yunten N. Isolated pontine infarction due to rhinocerebral mucormycosis. Neuroradiology 1999;41(03):179–181

58 Groppo ER, El-Sayed IH, Aiken AH, Glastonbury CM. Computed tomography and magnetic resonance imaging characteristics of acute invasive fungal sinusitis. Arch Otolaryngol Head Neck Surg 2011;137(10):1005–1010